Laser and Particle Beams (2017), *35*, 397–408.
© Cambridge University Press, 2017 0263-0346/17
doi:10.1017/S0263034617000350

Numerical modelling of the cluster targets for their optimization in femtosecond-laser-cluster-driven experiments

A.S. BOLDAREV,[1,2] A.Y. FAENOV,[3,4] Y. FUKUDA,[5] S. JINNO,[6] T.A. PIKUZ,[4,7] M. KANDO,[5] K. KONDO,[5] AND R. KODAMA[3,7,8,9]

[1]Keldysh Institute of Applied Mathematics RAS, Moscow, Russia
[2]National Research Nuclear University MEPhI (Moscow Engineering Physics Institute), Moscow, Russia
[3]Open and Transdisiplinary Research Initiatives, Osaka University, Suita, Osaka 565-0871, Japan
[4]Joint Institute for High Temperatures, Russian Academy of Science, Moscow, 125412, Russia
[5]Kansai Photon Research Institute, National Institutes for Quantum and Radiological Science and Technology, Kizugawa, Kyoto, Japan
[6]Nuclear Professional School, The University of Tokyo, 2-22 Shirakata Shirane, Tokai, Naka, Ibaraki 319-1188, Japan
[7]Graduate School of Engineering, Osaka University, Suita, Osaka 565-0871, Japan
[8]Photon Pioneers center, Osaka University, Suita, Osaka 565-0871, Japan
[9]Institute of Laser Engineering, Osaka University, Suita, Osaka 565-0871, Japan

(RECEIVED 29 April 2017; ACCEPTED 12 May 2017)

Abstract

The interaction of femtosecond ultra-intense laser pulses with clusters increases absorption of the incident laser light compared with the interaction with solid targets and leads to enhanced generation of different quantum beams with unique parameters. Future investigations of such interaction urgently need detailed modeling and optimization of cluster parameters, for instance, in order to obtain the clusters with desired size, or some specific spatial configuration of the target etc. A numerical model of gas-cluster targets production by the nozzle flows of gases and binary mixtures is presented. Some previous results of the model utilization are summarized, and some new results are given. Techniques of experimental verification of the numerical results are discussed.

Keywords: Ultra-intense femtosecond laser–clusters interaction; Cluster targets; Numerical modelling; Nozzle flow; Kinetics of clusterization

1. INTRODUCTION

Investigations of the interaction of ultra-intense femtosecond laser radiation with solid and gas media have become especially important in recent years due to the possibility of investigations of fundamental properties of matter in extreme conditions and allow one to use new approaches for solving a number of application issues. One of the rather widely used types of targets for the ultrashort laser pulses irradiation is the cluster targets, where a gas expanding through a supersonic nozzle forms a jet with some liquid (or solid) phase inclusions (clusters) (Hagena, 1992; Ditmire *et al.*, 1996, 1997, 1998, 1999; Dobosz *et al.*, 1998, 1999; Tajima *et al.*, 1999; Parra *et al.*, 2000, 2003; Rusek *et al.*, 2000; Abdallah *et al.*, 2001, 2003; Blasco *et al.*, 2001; Boldarev *et al.*, 2001, 2004, 2006; Faenov *et al.*, 2001, 2008, 2009, 2012, 2013, 2016*a*, *b*; Junkel-Vives *et al.*, 2002*a*, *b*; Skobelev *et al.*, 2002*a*, *b*; Dorchies *et al.*, 2003; Fukuda *et al.*, 2003, 2004*a*, *b*, 2008, 2009, 2013; Kim *et al.*, 2003, 2006; Hansen *et al.*, 2005; Gavrilenko *et al.*, 2006; Sherrill *et al.*, 2006; Davis *et al.*, 2007; Colgan *et al.*, 2008, 2011; Kugland *et al.*, 2008; Berkelbach *et al.*, 2009; Gasilov *et al.*, 2009; Pikuz *et al.*, 2009; Hayashi *et al.*, 2010, 2011; Zhang *et al.*, 2011, 2012; Bussolino *et al.*, 2013; Chen *et al.*, 2013; Jinno *et al.*, 2013*a*, *b*; Oks *et al.*, 2014, 2015; Koester *et al.*, 2015; Tao *et al.*, 2016). With this type of target it is possible to combine the advantages of solid (high density) and gas (debris-free, easy regeneration) targets. Due to the increased absorption, these targets are heated significantly, leading to enhanced generation of various radiation and particle beams (which are usually referred to as quantum beams). Indeed, very promising results have been obtained in experiments with this type of targets for various

Address correspondence and reprint request to: A.S. Boldarev, Keldysh Institute of Applied Mathematics RAS, Miusskaya sq. 4, Moscow, 125047, Russian Federation. E-mail: boldar@imamod.ru

https://doi.org/10.1017/S0263034617000350 Published online by Cambridge University Press

applications, including nuclear fusion (Ditmire *et al.*, 1999), X-ray emission (Parra *et al.*, 2000, 2003; Abdallah *et al.*, 2001, 2003; Junkel-Vives *et al.*, 2002*a*, *b*; Fukuda *et al.*, 2003, 2004*a*, *b*, 2008; Hansen *et al.*, 2005; Kim *et al.*, 2006; Sherrill *et al.*, 2006; Colgan *et al.*, 2008; Kugland *et al.*, 2008; Berkelbach *et al.*, 2009; Gasilov *et al.*, 2009; Pikuz *et al.*, 2009; Hayashi *et al.*, 2010, 2011; Zhang *et al.*, 2011; Faenov *et al.*, 2013), betatron X-ray radiation (Chen *et al.*, 2013), laser-driven ion acceleration (Dobosz *et al.*, 1998, 1999; Kim *et al.*, 2006; Faenov *et al.*, 2009, 2013, 2016*b*; Fukuda *et al.*, 2009, 2013), laser-cluster-driven electron acceleration (Zhang *et al.*, 2012; Bussolino *et al.*, 2013; Faenov *et al.*, 2013, 2016*b*; Koester *et al.*, 2015) and so on.

In contrast with the solid and gaseous targets, for a cluster target it is difficult to estimate the initial (before laser pulse) state, namely, the concentration and the mean size of the clusters, their dispersion etc. Since the processes of clusters formation in a gas jet are complex, there cannot be a simple estimation procedure, which would give adequate results in all cases. One of the most frequently used approaches is the heuristic scaling theory by Hagena (1992), where the mean cluster size (the mean number of atoms in a cluster) is given by formula

$$\langle N\rangle = 33\left(\frac{\Gamma^*}{1000}\right)^{2.35} \quad (\text{for } \Gamma^* > 1000), \tag{1}$$

where the parameter Γ^* is supposed to define completely the process of clusterization and is given by

$$\Gamma^* = k_\text{h}\left(\frac{0.74d}{\tan\alpha}\right)^{0.85} P_0 T_0^{-2.29}, \tag{2}$$

where $k_\text{h} = 1650$ for argon and $k_\text{h} = 2890$ for krypton, d is the critical diameter of the nozzle in micrometers, P_0 and T_0 are initial pressure and temperature of the gas (in millibars and kelvins, respectively), α is the half-angle of the nozzle expansion.

In these expressions one can see that the geometry of the nozzle is taken into account in the form of only two parameters – critical diameter d and the half-angle α of expansion. The properties of the working gas are represented by only one number k_h. Besides, this theory does not give the spatial distribution of the gas-cluster jet. So, this theory can be valid for a restricted range of variants – conical nozzles, argon and krypton as working gas. Nevertheless, this theory is widely used because it is simple and easy for use, it became a tradition to compare results of other clusters evaluation procedures with it.

To obtain more reliable data for wide range of variants (e.g., nozzle shapes, working gases and initial gas conditions) some experimental procedures were developed. Commonly, one uses the interferometric measurements to obtain the average density of the jet, and the Rayleigh scattering technique to obtain the clusters parameters, (Dorchies *et al.*, 2003; Kim *et al.*, 2003; Tao *et al.*, 2016). Rayleigh scattering signal is proportional to $n_\text{c}\langle N^2\rangle \approx (1-\beta)n_\text{a}\langle N\rangle$, where n_c and n_a are concentrations of clusters and atoms (or molecules for molecular gases), N is the number of atoms (molecules) in a cluster, β is the mass fraction of the gas phase in the gas-cluster jet. Along with the atomic concentration n_a given from the interferometry, that makes possible to define two parameters among three independent ones: β, n_c and $\langle N\rangle$, so, some additional information is needed to achieve the complete information about the clusterized medium. In Kim *et al.* (2003) it is supposed that $1-\beta$ is a value of order of 1, so, assuming $\beta = 0$, we do not produce an error higher than several times. In Tao *et al.* (2016) the value β is taken from the numerical modelling.

For large (submicron-sized) clusters (which were obtained by the use of specially designed nozzle) it is possible to utilize Mie scattering technique instead of Rayleigh scattering (Jinno *et al.*, 2013*a*, *b*). This allows to obtain directly the mean cluster size and its standard deviation (but in assumption that the clusters distribution over their sizes is lognormal).

Another method to explore cluster targets is the numerical modelling. A mathematical model based on the representation of clusters as spherical microdroplets and on the kinetic theory of Frenkel (1955), Abraham (1974) was proposed by Boldarev *et al.* (2004, 2006). Later this model was generalized to take into account the binary mixtures of gases where one component does not form clusters (Jinno *et al.*, 2013*b*). According to the results of the modelling, it is turned out that the binary mixtures can provide high degree of clusterization of the clusterizing component, while the gas between clusters consists almost of the inert component. That was very convenient for the soft X-ray production when the intercluster gas can absorb a considerable part of the X-ray radiation produced by clusters illuminated by the laser pulse; in the case of $He + CO_2$ mixture helium does not absorb the radiation (Fukuda *et al.*, 2008; Gasilov *et al.*, 2009; Pikuz *et al.*, 2009).

2. NUMERICAL MODEL OF THE CLUSTERIZATION IN NOZZLE FLOWS OF BINARY MIXTURES

We consider a gas mixture with two components: inert (which we denote by index i) and clusterizing, or condensing one (denoted by index c). The condensing component, in turn, is subdivided into gas phase (index g) and liquid (or condensed) one, denoted by index l. So, we have, in fact, three components of our medium: inert component i, condensing gas cg and clusters cl.

Since we assume that the clusters are comparatively small and do not move with respect to the surrounding gas, we may consider the composition of our mixture (namely, mass or molar relation between i and c components) to be constant

https://doi.org/10.1017/S0263034617000350 Published online by Cambridge University Press

and known. So, we introduce the value φ as the mass fraction of the condensing component. So, we can write for the densities of the components

$$\rho_c = \varphi\rho, \quad \rho_i = (1-\varphi)\rho.$$

We introduce also the so-called *dryness degree* β, which is the mass fraction of the *cg* subcomponent in the whole *c* component. So, we can also write

$$\rho_{cg} = \beta\rho_c = \beta\varphi\rho, \quad \rho_{cl} = (1-\beta)\rho_c = (1-\beta)\varphi\rho,$$

$$\rho_i = (1-\varphi)\rho.$$

In these expressions ρ_{cg}, ρ_{cl}, and ρ_i are densities of the components of the mixture, that is mass of a component per single volume of the whole mixture. Since the volume of the clusters is negligibly small, for the gas components these are also the densities of these components themselves, which appear in all thermodynamic relations for this component. For the clusters, of course, ρ_{cl} is much smaller than the density of the liquid phase itself, which we denote as ρ_l^0.

The process of clusters formation is described in kinetics terms and, of course, this process is essentially nonequilibrium. But we consider two *gas* components *i* and *cg* to be in thermodynamic equilibrium with each other. So, we suppose that the temperature of two components of the gas phase is the same $T_i = T_{cg} = T$ (and may differ from the temperature of the clusters T_{cl}). Another supposition is that the pressure of the mixture, in accordance with Dalton law, is the sum of the partial pressures of the gaseous components, $P = P_i + P_{cg}$. The liquid phase does not render the pressure, since it is not continuous.

These suppositions allow us to consider the density and internal energy of the whole mixture, not of the individual components. So, the governing system of equations practically does not differ from the single-gas case:

$$\frac{\partial\rho}{\partial t} + \operatorname{div}(\rho\mathbf{v}) = 0, \tag{3}$$

$$\frac{\partial\rho\mathbf{v}}{\partial t} + \operatorname{div}(\rho\mathbf{v}\mathbf{v}) = -\operatorname{grad} P, \tag{4}$$

$$\frac{\partial}{\partial t}\left(\rho\varepsilon + \rho\frac{\mathbf{v}^2}{2}\right) + \operatorname{div}\left(\rho\mathbf{v}\left(\varepsilon + \frac{\mathbf{v}^2}{2}\right)\right) = -\operatorname{div} P\mathbf{v}, \tag{5}$$

$$\frac{\partial\rho\Omega_n}{\partial t} + \operatorname{div}(\rho\mathbf{v}\Omega_n) = Ir_*^n + \dot{r}n\rho\Omega_{n-1}, \quad n = 0, 1, 2, \tag{6}$$

$$\frac{\partial\rho\beta}{\partial t} + \operatorname{div}(\rho\mathbf{v}\beta) = -\frac{4}{3}\frac{\pi\rho_l^0 Ir_*^3}{\varphi} - \frac{4\pi\rho\rho_l^0\dot{r}\Omega_2}{\varphi}. \tag{7}$$

Here Ω_n are the moments of the distribution function of the clusters with respect to their radii:

$$\rho\Omega_n = \int_0^\infty r^n f(r, \mathbf{x}, t)\, dr.$$

So, we can write for the third moment

$$1 - \beta = \frac{4}{3}\frac{\rho_l^0\pi\Omega_3}{\varphi}.$$

We use the same model of kinetics of the phase transitions as in the single-gas case, but with taking into account the presence of the inert component. The inert component changes the gasdynamics parameters but does not take part in the clusters origination process itself. To close the system (3)–(7), we use the following relationships. The critical radius

$$r_* = \frac{2\sigma(T)}{\rho_l^0 RT\ln(P_{cg}/P_s(T))}. \tag{8}$$

The nucleation rate

$$I = \frac{1}{\rho_l^0}\sqrt{\frac{2\sigma(T)\mu}{\pi N_A}}\left(\frac{P_{cg}}{kT}\right)^2\exp\left(-\frac{4\pi\sigma(T)r_*^2}{3kT}\right). \tag{9}$$

The rate of clusters growth

$$\dot{r} = \frac{P_{cg}}{\rho_l^0\sqrt{2\pi RT}}\left(1 - \sqrt{\frac{T}{T_s(P_{cg})}}\right). \tag{10}$$

The model includes also some thermodynamic relationships, which express the properties of the working gas and close the system of equations. To close the system, we need expressions $P(\rho, \varepsilon, \beta)$, $T(\rho, \varepsilon, \beta)$ and the expressions for some values at the saturation line. In the single-gas model we used expressions

$$P = P(\rho, \varepsilon, \beta) = \rho\frac{\varepsilon + (1-\beta)L_s}{\gamma/(\beta(\gamma-1)) - 1}, \quad T = \frac{P}{\beta Z\rho R}, \tag{11}$$

which are the consequences of the simple equation of state of the ideal gas and the relationships between the heat of phase transition and the enthalpies of the phases,

$$L_s = H_g - H_l.$$

In the gas mixture model, we apply (11) to each of the components *i* and *c*. As a result, instead of direct expressions (11) we obtain a system of algebraic equations, which includes (11) for both components, equality of the temperatures of the components and the relationship between the specific internal energies of the components:

$$\varepsilon = (1-\varphi)\varepsilon_i + \varphi\varepsilon_c.$$

https://doi.org/10.1017/S0263034617000350 Published online by Cambridge University Press

3. EXPERIMENTAL VERIFICATION OF THE MODEL

This numerical model is based on some suppositions, which are sometimes not convincing. The main objection to this model is that it operates with the thermodynamic approach when considering the critical nuclei of the clusters. Besides, the thermodynamic properties of the working gas are not known precisely, because the origination of clusters takes place in a supercooled metastable gas. So, an experimental verification of the numerical results obtained by this model was needed.

An indirect experimental confirmation of the adequateness of the numerical model (its version for the pure gas) was given when we designed special three-staged conical nozzle (Boldarev *et al.*, 2006) for obtaining large (submicron-sized) clusters. The large clusters were needed to diminish the prepulse influence for low-contrast laser pulses (Fukuda *et al.*, 2004*a*). The nozzle had three conical stages, the first one expanded from diameter 0.5 to 0.7 mm at the length of 29 mm, the second stage expanded from 0.7 to 0.8 mm at the length 30 mm, and the last stage of length 16 mm had the outlet diameter 2 mm. Such a nozzle geometry was chosen on the base of numerical modelling for argon at initial pressure 60 bar. Although initially there were no direct measurement of the cluster sizes, in Fukuda *et al.* (2004*a*) a good correlation was observed between the X-ray intensity measured in the experiment and the mean cluster size obtained from the modelling.

The submicron size of the clusters allowed to apply Mie scattering technique instead of usual Rayleigh scattering one (Jinno *et al.*, 2013*a*, *b*). In these works, the binary mixtures $He(90\%) + CO_2(10\%)$ and $H_2(70\%) + CO_2(30\%)$ at initial pressure 60 bar were used. For the above described three-staged nozzle, the computations gave the mean cluster size 0.360 and 0.588 μm respectively, and the standard deviation was 0.072 and 0.090 μm for these two gas mixtures, respectively. By applying Mie scattering technique, the experimental measurements of the average cluster size were performed, and they gave 0.26 ± 0.04 μm (S.D. 0.08 ± 0.01 μm) and 0.28 ± 0.03 μm (S.D. 0.13 ± 0.02 μm), respectively. So, there is about twofold discrepancy between experimental and numerical results. It should be noted that a twofold difference in cluster diameter corresponds to the difference of an order of magnitude with respect to the volume and, respectively, the number of atoms (molecules).

A systematic comparison of the clusters parameters obtained from the numerical modelling with ones given from the experiment have recently been performed in Tao *et al.* (2016). The authors of that paper explored the mathematical models of clusters formation very similar to (3)–(11), but with more reliable thermodynamic completion. In the frames of the model, some questions arise, like, for instance, what temperature should be ascribed to a cluster nucleus which appears in the supercooled gas – the temperature of the surrounding gas or the saturation temperature at the given pressure. Depending on the answer to this and other similar questions, one obtains different variations of the model, whose results dramatically differ from each other. In fact, there are no comprehensive and definite answers to that questions, since they are based on the supposition of applicability of the thermodynamical approach to the arising clusters nuclei.

On the base of comparison of numerical data and the experimental results, in Tao *et al.* (2016) a single (referred to as baseline) model variation have been chosen, for which the results were the most close to the experiment. For this model, a discrepancy was still of an order of magnitude, that is similar to one observed in Jinno *et al.* (2013*a*, *b*). It should be noted that in Tao *et al.* (2016) some other experimental conditions were considered, they used argon as a working gas and another nozzle shape. Under these conditions, there were not expected large clusters, so, the usual experimental technique based on interferometry along with Rayleigh scattering was applied. The missing third parameter was taken from the numerical modeling – it was noticed that the dryness degree β, in contrast with the clusters size, does not depend on the model variations. That conclusion could be expected, since the dryness degree is a characteristics of the thermodynamical equilibrium state, it must not depend on the kinetic processes of clusters nuclei origination, which affect such parameters as clusters size and concentration.

In order to compare our model (3)–(11) with the baseline model proposed in Tao *et al.* (2016), we performed modeling of the variants considered in Tao *et al.* (2016) with our model. According to Tao *et al.* (2016), the planar nozzle with throat width of 0.22 mm, total length of 10 mm and half-angle of divergence of 14° was taken, the working gas was argon. Two series of variants were computed, in the pressure series the temperature was 293 K while the pressure varied from 10 to 100 bar. In the temperature series the pressure was constant and equal to 50 bar, while temperature varied from 200 to 350 K. A particular variant in pressure or temperature series may be characterized by its pressure or temperature value P_0 or T_0, but in Tao *et al.* (2016) the variants were characterized by the Hagena parameter Γ^* (2), which is a function of P_0 and T_0. In fact, Γ^* is not used in our model and in the models described in Tao *et al.* (2016), so, there is no physical sense in such a characterization, it is merely a question of representation of the results. Moreover, the parameter Γ^* was introduced for conical nozzles, while the paper (Tao *et al.*, 2016) considers the planar ones. But we keep this characterization for our computational results in order to compare them with ones from Tao *et al.* (2016). Besides, arranging the results in the form of dependence on Γ^* allows us to represent the results of both series, pressure and temperature, on the same plot, see Figures 1–3. But it could be easily seen that the pressure and temperature series show different dependence of the computed parameters on Γ^*; that demonstrates once more that the parameter Γ^* seems not to have a physical relevance, and it cannot, in general, be considered as the only parameter, which defines entirely the clusterization process.

https://doi.org/10.1017/S0263034617000350 Published online by Cambridge University Press

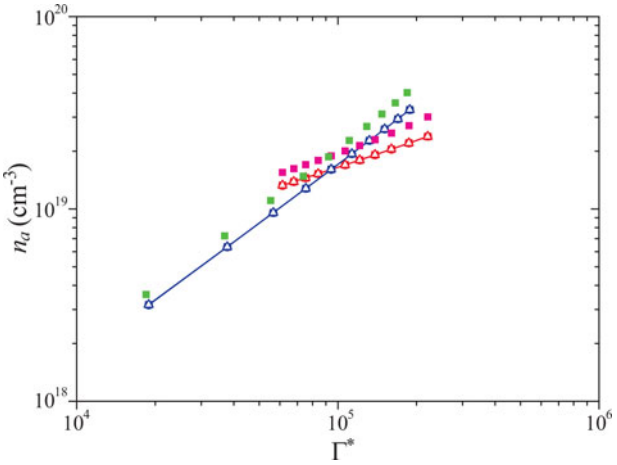

Fig. 1. Total atom number density n_a as a function of the Hagena parameter Γ* at the exit of the nozzle. The hollow symbols and lines correspond to the results of Tao *et al.* (2016), the blue ones are for the pressure series (the initial pressure P_0 varies from 10 to 100 bar at the constant initial temperature $T_0 = 293$K), the red ones are for the temperature series (the initial temperature T_0 varies from 200 to 350 K at the constant initial pressure $P_0 = 50$ bar). Green and purple solid squares are the results of our model (3)–(11), pressure and temperature series, respectively. A good agreement between both theories is clearly seen.

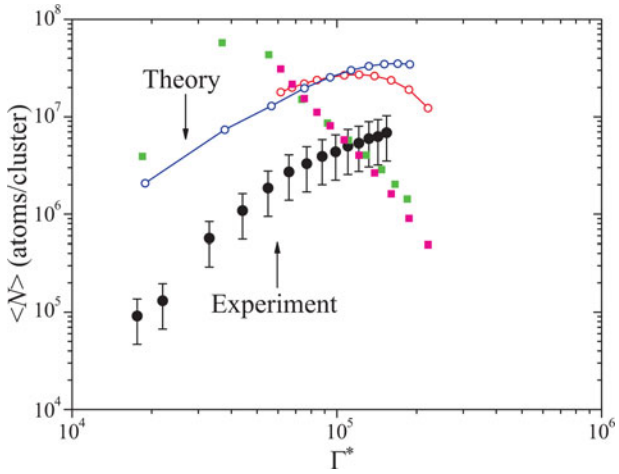

Fig. 3. Average number of atoms per cluster $\langle N \rangle$ as a function of the Hagena parameter Γ* at the exit of the nozzle. The hollow circles and lines correspond to the results of Tao *et al.* (2016), the blue ones are for the pressure series (the initial pressure P_0 varies from 10 to 100 bar at the constant initial temperature $T_0 = 293$K), the red ones are for the temperature series (the initial temperature T_0 varies from 200 to 350 K at the constant initial pressure $P_0 = 50$ bar). Green and purple solid squares are the results of our model (3)–(11), pressure and temperature series respectively. The black circles represent the experimental data of Tao *et al.* (2016) obtained for various pressures at the initial temperature $T_0 = 293$K.

At Figures 1–3 the results of the 1D computations are presented. The blue and red lines and hollow symbols are taken from Tao *et al.* (2016) and correspond to the results of the baseline model, pressure, and temperature series, respectively. The results of our model (3)–(11) are depicted as green (the pressure series) and purple (the temperature series) solid squares. Besides, the experimental results (Tao *et al.*, 2016) are represented at Figure 3 as solid black circles and error bars.

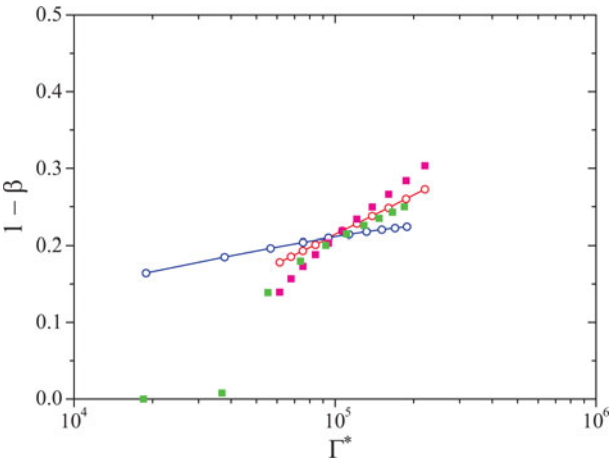

Fig. 2. Liquid mass fraction 1 − β as a function of the Hagena parameter Γ* at the exit of the nozzle. The hollow circles and lines correspond to the results of Tao *et al.* (2016), the blue ones are for the pressure series (the initial pressure P_0 varies from 10 to 100 bar at the constant initial temperature $T_0 = 293$K), the red ones are for the temperature series (the initial temperature T_0 varies from 200 to 350 K at the constant initial pressure $P_0 = 50$ bar). Green and purple solid squares are the results of our model (3)–(11), pressure and temperature series, respectively. A good agreement between both theories is clearly seen.

The parameters n_a and β, which are shown in Figures 1 and 2, are defined by gasdynamic and thermodynamical processes, they are not affected by the kinetic processes of the clusters origination. In Tao *et al.* (2016) these parameters practically do not depend on the model variation. Nevertheless, difference in the thermodynamic completion of the models [our (3)–(11) and (Tao *et al.*, 2016)] leads to some considerable discrepancy in these values.

As for the values influenced by kinetic processes, like average cluster size, the difference between the baseline model (Tao *et al.*, 2016) results and ones of our model (3)–(11) is more noticeable, see Figure 3. As it was mentioned in Tao *et al.* (2016), there is an inverse dependence of cluster size on the Hagena parameter Γ* for our model (3)–(11). For some variants (and range of Γ*) the results of the model (3)–(11) correspond to the data obtained from the baseline model (Tao *et al.*, 2016) and to the experimental data, within their divergence of an order of value.

Results of the comparison of the numerical and experimental data, presented in Figure 3, shows that both models, our one (3)–(11) and the baseline one from Tao *et al.* (2016), give an error of an order of magnitude for $\langle N \rangle$ value. As it is mentioned above, that was the case also for our model applied to experimental variants (Jinno *et al.*, 2013*a*, *b*). By now, numerical models do not give higher accuracy in the cluster size prediction. That may be explained by the above mentioned principal drawback of the clusterization models – they apply the thermodynamic approach to metastable states of the gas and to very tiny objects like the

https://doi.org/10.1017/S0263034617000350 Published online by Cambridge University Press

clusterization nuclei, which should be adequately described on the molecular level. On the other hand, we cannot rely completely on the accuracy of the experimental techniques of the cluster size measurement. There may be other possible reasons why such a discrepancy exists between modeling and experimentally obtained data. One of them connected with the fact that it is impossible to produce nozzle with ideal shape and ideally smoothed surface without any roughness. It means that even in the case of absolutely correct modeling of cluster media some discrepancy should exist. Additionally, in femtosecond laser-cluster experiments nozzle is strongly influenced by the X-ray radiation and various particles and eventually it starts to have a rough surface, which should also cause additional discrepancy between experimentally measured sizes of clusters and modeled ones.

4. SOME RECENT COMPUTATIONS WITH THE MODEL

4.1. Micronozzles

The submillimeter-sized nozzles with the gas at very high pressures (about 100–200 bar) were investigated. Approximate parameters of these nozzles were taken from Sylla *et al.* (2012). Although in that article there are no detailed descriptions of the nozzle geometry, it was very interesting to check our model by variants with very high pressures, since we have never performed the modelling for high pressure values and small nozzle sizes.

The conical nozzles with diameters 300–400 and 100–400 μm, and the length 1 or 2 mm were taken, with CO_2 gas at total pressure 40 bar and argon at 100 and 200 bar. The Figures 4 and 5 represent the distributions of some values along the nozzle obtained in the computations.

The modelling gives very low (about 0.02 μm) average cluster size for this type of nozzle. That may be expected, taking into account high divergence angle. Also one can see that the longer nozzle ($L = 2$ mm) gives bigger clusters than the shorter one ($L = 1$ mm), but the fraction of clusterized medium $1 - \beta$ is the same for both nozzles. That confirms the above statement that n_a and β are defined only by gasdynamical and thermodynamical processes, and consequently depend only on the total expansion of the nozzle, while the cluster size is influenced by kinetic processes, and, the less is the expansion rate, the higher is the cluster size.

4.2. Cooled hydrogen

The aim of this modelling was to evaluate the clusters parameters in the experiment with cooled molecular hydrogen and the

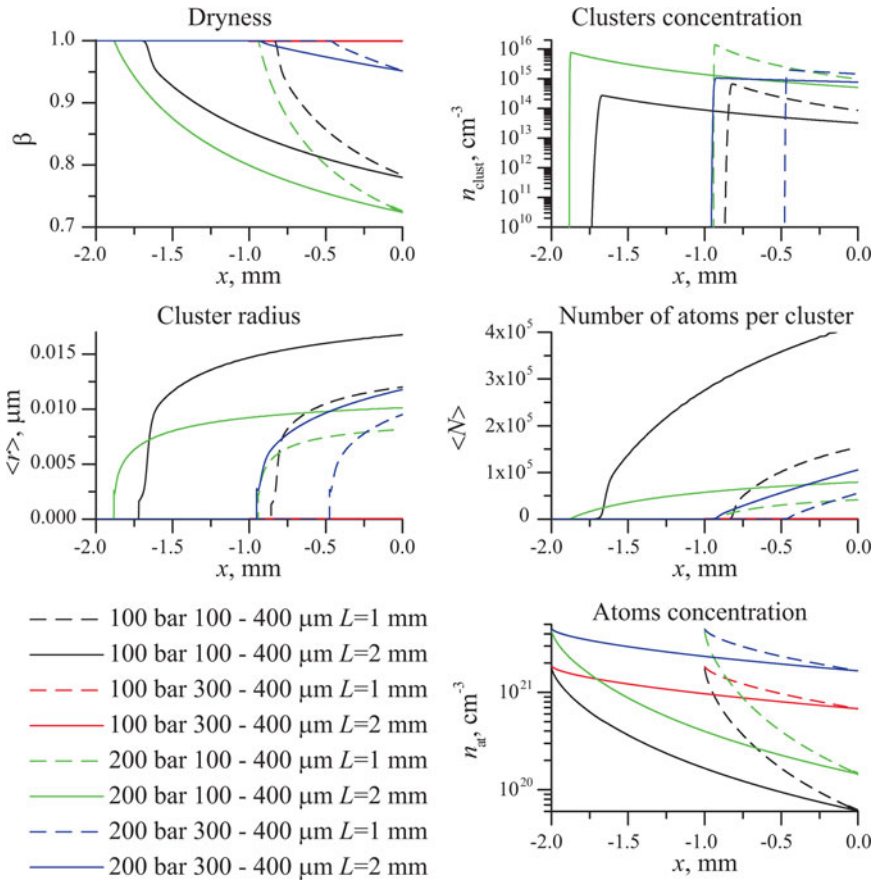

Fig. 4. Computed distributions of some values along the micronozzles for argon.

https://doi.org/10.1017/S0263034617000350 Published online by Cambridge University Press

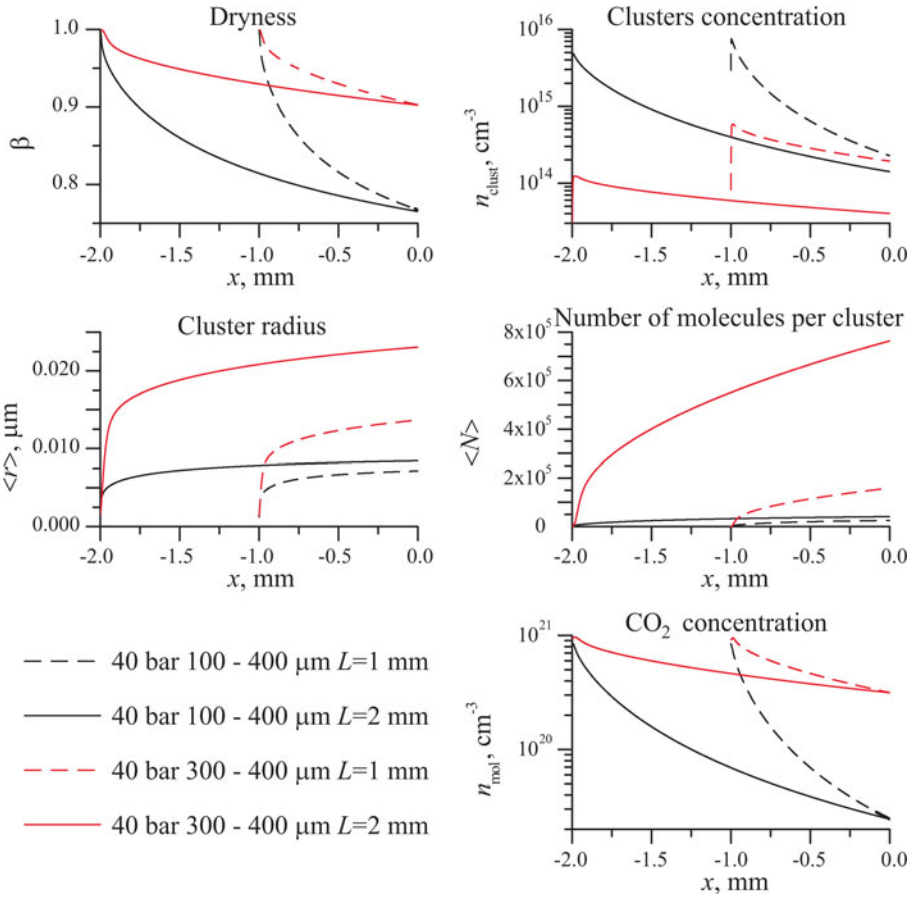

Fig. 5. Computed distributions of some values along the micronozzles for CO_2.

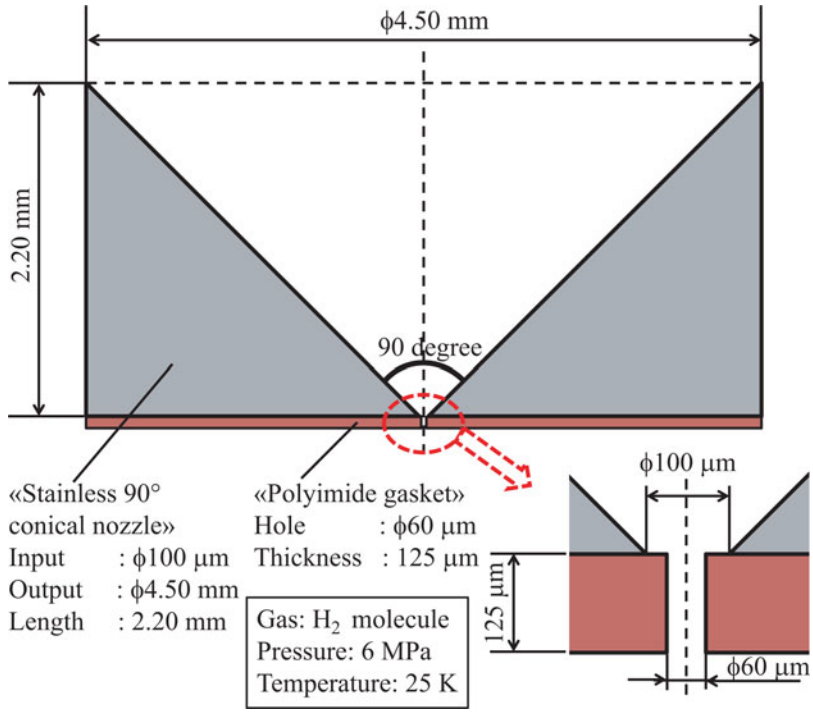

Fig. 6. The nozzle used in experiments.

https://doi.org/10.1017/S0263034617000350 Published online by Cambridge University Press

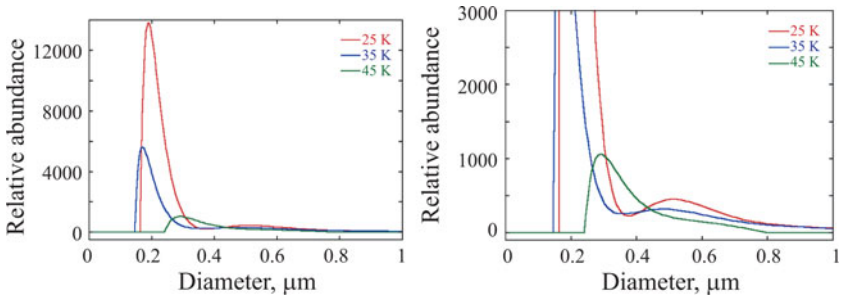

Fig. 7. Experimental size distribution of H_2 clusters obtained by Mie scattering measurements (different scales on the left and right plots).

90° nozzle is shown in Figure 6. With the molecular hydrogen at initial pressure 60 bar and temperatures 25, 35, and 45 K, Mie scattering measurements have shown the presence of comparatively large (~0.2 μm diameter) clusters, see Figure 7.

According to the thermodynamical properties of hydrogen (which are available, for example, at the site http://webbook.nist.gov/chemistry/fluid/), the hydrogen at 60 bar and 25 K is liquid, and it seemed to be very doubtful that this was the exact initial parameters of the gas. As for the temperatures 35 and 45 K, the state of the hydrogen is marked as "supercritical", but the isentropic lines starting from these points [i.e., (60 bar, 35 K) and (60 bar, 45 K)] do not intersect the saturation line. They enter the liquid area higher than the critical point. So, the expansion of the hydrogen in a nozzle cannot lead to the phase transition. That may mean that the clusterization in that case takes place because of some other processes – for example, inhomogeneous expansion of initially dense fluid medium.

More probable thing is that the temperature values 25, 35, and 45 K do not correspond to actual gas temperature. In the experimental setup, the valve was cooled (till the given temperatures), but the temperature of the gas remained unknown. So, it was decided to perform the modeling for the initial temperatures in the range 50–180 K.

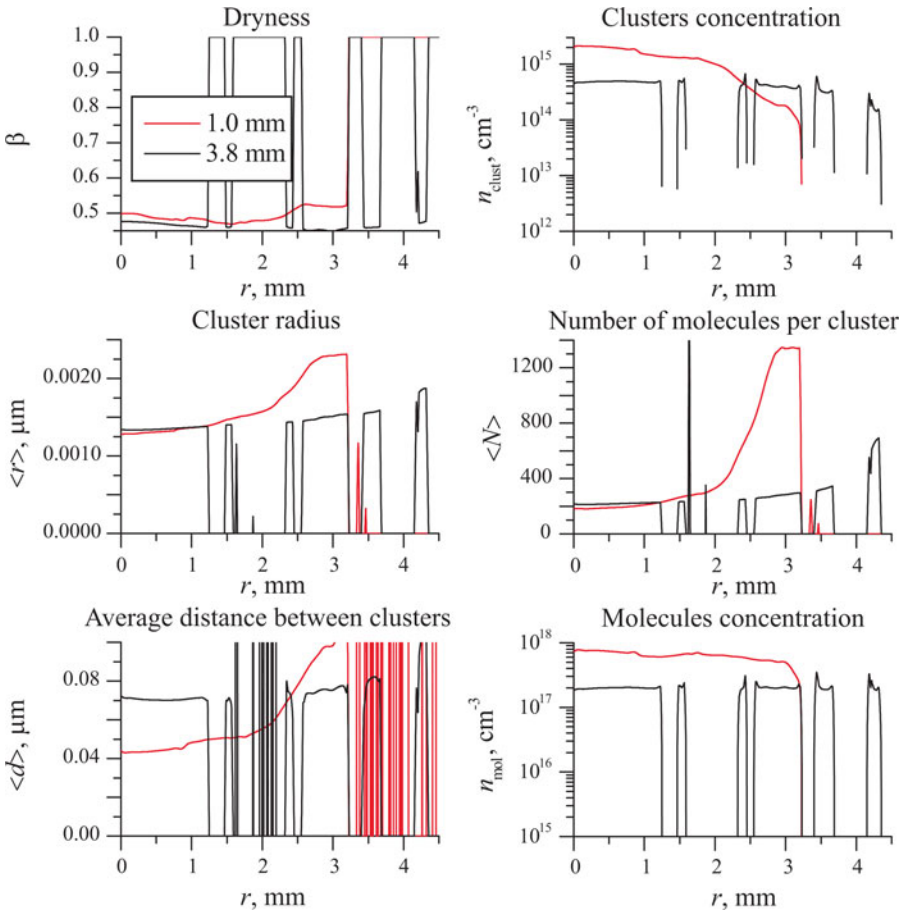

Fig. 8. Computed spatial distributions of clusters parameters at the distances 1 and 3.8 mm from the nozzle outlet.

https://doi.org/10.1017/S0263034617000350 Published online by Cambridge University Press

Because of high expansion angle of the nozzle, the modelling was performed in the 2D formulation. There were taken 11 variants with different temperatures. No clusterization was observed, except for the variant for initial temperature 50 K. The results for 60 bar and 50 K are shown in Figure 8.

Some oscillations of the curve corresponding to the far section (3.8 mm from the nozzle) can be explained by the interaction of the highly-expanded gas jet with the "background" gas, which was taken only for the computations. It was possible to decrease the density of that "background" gas, and the oscillations in that case can be eliminated, but we still have the reliable parameters distribution in the vicinity of the nozzle's axis.

The results of numerical modelling show very high clusterization degree (the mass fraction of the clusterized gas) of 50%, which never has been achieved for the pure gases. But the average cluster size is very low – this result is expected because of very high divergence angle of the nozzle, but do not correspond to the experimental data (Fig. 7).

5. CONCLUSIONS

The numerical modelling became an important source of information about the cluster target parameters. The model (3)–(11) usually gave a qualitative correspondence with experimental data and allowed to understand what one can expect in performing experiments with a particular configuration (nozzle geometry, working gas, and its initial parameters). The results obtained with such a nozzle allowed to provide optimization of nozzles for generation of intensive quantum beams in femtosecond laser-cluster driven experiments [see results obtained in (Rusek *et al.*, 2000; Abdallah *et al.*, 2001, 2003; Blasco *et al.*, 2001; Boldarev *et al.*, 2001; Junkel-Vives *et al.*, 2002*b*; Skobelev *et al.*, 2002*a*, *b*; Fukuda *et al.*, 2003, 2004*a*, 2008, 2009, 2013; Sherrill *et al.*, 2006; Colgan *et al.*, 2008, 2011; Faenov *et al.*, 2008, 2009, 2012, 2013, 2016*b*; Berkelbach *et al.*, 2009; Pikuz *et al.*, 2009; Hayashi *et al.*, 2010, 2011; Bussolino *et al.*, 2013; Oks *et al.*, 2014, 2015; Koester *et al.*, 2015)]. In last years, when the experimental technique of clusters parameters measurement has been developed (Jinno *et al.*, 2013*a*, *b*), it became clear that further development of the numerical models are required in order to obtain more precise quantitative correspondence.

ACKNOWLEDGMENTS

The work was supported by RFBR projects 15-01-06195_a and 16-29-15081_ofi_m, and was partially supported by the Academic Excellence Project of the NRNU MEPhI under contract with the Ministry of Education and Science of the Russian Federation No. 02.A03.21.0005. Also the work is supported by RAS Presidium Program for Basic Research No. 11 and by the Grant-in-Aid for Scientific Research (A) No. 26247100 by JSPS.

REFERENCES

Abdallah Jr., J., Csanak, G., Fukuda, Y., Akahane, Y., Aoyama, M., Inoue, N., Ueda, H., Yamakawa, K., Faenov, A.Y., Magunov, A.I., Pikuz, T.A. & Skobelev, I.Y. (2003). Time-dependent Boltzmann kinetic model of x-rays produced by ultrashort-pulse laser irradiation of argon clusters. *Phys. Rev. A* **68**, 063201.

Abdallah Jr., J., Faenov, A.Y., Skobelev, I.Y., Magunov, A.I., Pikuz, T.A., Auguste, T., D'Oliveira, P., Hulin, S. & Monot, P. (2001). Hot-electron influence on the x-ray emission spectra of Ar clusters heated by a high-intensity 60-fs laser pulse. *Phys. Rev. A* **63**, 032706.

Abraham, F.F. (1974). *Homogeneous Nucleation Theory*. New York: Academic.

Berkelbach, T.C., Colgan, J., Abdallah Jr., J., Faenov, A.Y., Pikuz, T.A., Fukuda, Y. & Yamakawa, K. (2009). Modeling energy dependence of the inner-shell x-ray emission produced by femtosecond-pulse laser irradiation of xenon clusters. *Phys. Rev. E* **79**, 016407.

Blasco, F., Stenz, C., Salin, F., Faenov, A.Y., Magunov, A.I., Pikuz, T.A. & Skobelev, I.Y. (2001). Portable, tunable, high-luminosity spherical crystal spectrometer with an x-ray charge coupled device, for high-resolution x-ray spectromicroscopy of clusters heated by femtosecond laser pulses. *Rev. Sci. Instrum.* **72**, 1956.

Boldarev, A.S., Gasilov, V.A., Blasco, F., Stenz, C., Dorchies, F., Salin, F., Faenov, A.Y., Pikuz, T.A., Magunov, A.I. & Skobelev, I.Y. (2001). Modeling cluster jets as targets for high-power ultrashort laser pulses. *JETP Lett.* **73**, 514–518.

Boldarev, A.S., Gasilov, V.A. & Faenov, A.Y. (2004). On the generation of large clusters in forming gas-jet targets for lasers. *Tech. Phys.* **49**, 388–395.

Boldarev, A.S., Gasilov, V.A., Faenov, A.Y., Fukuda, Y. & Yamakawa, K. (2006). Gas-cluster targets for femtosecond laser interaction: Modeling and optimization. *Rev. Sci. Instrum.* **77**, 083112.

Bussolino, G.C., Faenov, A., Giulietti, A., Giulietti, D., Koester, P., Labate, L., Levato, T., Pikuz, T. & Gizzi, L.A. (2013). Electron radiography using a table-top laser-cluster plasma accelerator. *J. Phys. D: Appl. Phys.* **46**, 245501.

Chen, L.M., Yan, W.C., Li, D.Z., Hu, Z.D., Zhang, L., Wang, W.M., Hafz, N., Mao, J.Y., Huang, K., Ma, Y., Zhao, J.R., Ma, J.L., Li, Y.T., Lu, X., Sheng, Z.M., Wei, Z.Y., Gao, J. & Zhang, J. (2013). Bright betatron X-ray radiation from a laser-driven-clustering gas target. *Sci. Rep.* **3**, 1912.

Colgan, J., Abdallah Jr., J., Faenov, A.Y., Pikuz, T.A., Skobelev, I.Y., Fortov, V.E., Fukuda, Y., Akahane, Y., Aoyama, M., Inoue, N. & Yamakawa, K. (2008). The role of hollow atoms in the spectra of an ultrashort-pulse-laser-driven Ar cluster target. *Laser Part. Beams* **26**, 83–94.

Colgan, J., Abdallah Jr., J., Faenov, A.Y., Pikuz, T.A., Skobelev, I.Yu., Fukuda, Y., Hayashi, Y., Pirozhkov, A., Kawase, K., Shimomura, T., Kiriyama, H., Kato, Y., Bulanov, S.V. & Kando, M. (2011). Observation and modeling of high resolution spectral features of the inner-shell X-ray emission produced by 10^{-10} contrast femtosecond-pulse laser irradiation of argon clusters. *High Energy Density Phys.* **7**, 77–83.

Davis, J., Petrov, J.M. & Velikovich, A. (2007). Nonlinear energy absorption of rare gas clusters in intense laser field. *Phys. Plasmas* **14**, 060701.

https://doi.org/10.1017/S0263034617000350 Published online by Cambridge University Press

Ditmire, T., Donnelly, T., Rubenchik, A.M., Falcone, R.W. & Perry, M.D. (1996). Interaction of intense laser pulses with atomic clusters. *Phys. Rev. A* **53**, 3379.

Ditmire, T., Gumbrell, E.T., Smith, R.A., Djaoui, A. & Hutchinson, M.H.R. (1998). Time-resolved study of nonlocal electron heat transport in high temperature plasmas. *Phys. Rev. Lett*. **80**, 720.

Ditmire, T., Tisch, J.W.G., Springate, E., Mason, M.B., Hay, N., Marangos, J.P. & Hutchinson, M.H.R. (1997). High energy ion explosion of atomic clusters: Transition from molecular to plasma behavior. *Phys. Rev. Lett*. **78**, 2732.

Ditmire, T., Zweiback, J., Yanovsky, V.P., Cowan, T.E., Hays, G. & Wharton, K.B. (1999). Nuclear fusion from explosions of femtosecond laser-heated deuterium clusters. *Nature* **398**, 489–492.

Dobosz, S., Schmidt, M., Perdrix, M., Meynadier, P., Gobert, O., Normand, D., Ellert, K., Blenski, T., Faenov, A.Y., Magunov, A.I., Pikuz, T.A., Skobelev, I.Y. & Andreev, N.E. (1999). Observation of ions with energies above 100 keV produced by the interaction of a 60-fs laser pulse with clusters. *JETP* **88**, 1122–1129.

Dobosz, S., Schmidt, M., Perdrix, M., Meynadier, P., Gobert, O., Normand, D., Faenov, A.Y., Magunov, A.I., Pikuz, T.A., Skobelev, I.Y. & Andreev, N.E. (1998). Characteristic features of the x-ray spectra of a plasma produced by heating CO_2 clusters by intense femtosecond laser pulses with $\lambda=0.8$ and 0.4 μm. *JETP Lett*. **68**, 485–491.

Dorchies, F., Blasco, F., Caillaud, T., Stevefelt, J., Stenz, C., Boldarev, A.S. & Gasilov, V.A. (2003). Spatial distribution of cluster size and density in supersonic jets as targets for intense laser pulses. *Phys. Rev. A* **68**, 023201.

Faenov, A.Y., Magunov, A.I., Pikuz, T.A., Skobelev, I.Y., Giulietti, D., Betti, S., Galimberti, M., Gamucci, A., Giulietti, A., Gizzi, L.A., Labate, L., Levato, T., Tomassini, P., Marques, J.R., Bourgeois, N., Dobosz-Dufrenoy, S., Ceccoti, T., Monot, P., Reau, F., Popoescu, H., D'Oliveira, P., Martin, P., Fukuda, Y., Boldarev, A.S., Gasilov, S.V. & Gasilov, V.A. (2008). Non-adiabatic cluster expansion after ultrashort laser interaction. *Laser Part. Beams* **26**, 69–82.

Faenov, A.Y., Oks, E., Dalimier, E., Skobelev, I.Y., Pikuz, S.A., Pikuz, T.A., Zhvaniya, I.A., Fukuda, Y., Andreev, A., Koga, J., Sakaki, H., Kotaki, H., Pirozhkov, A.S., Hayashi, Y., Kawachi, T., Kando, M., Kondo, K., Zhidkov, A.G. & Kodama, R. (2016*a*). X-ray spectral diagnostics of laser harmonic generation in the interaction of relativistic femtosecond laser pulses with clusters. *Quant. Electron*. **46**, 338–341.

Faenov, A.Y., Pikuz, T.A., Fukuda, Y., Kando, M., Kotaki, H., Homma, T., Kawase, K., Kameshima, T., Pirozhkov, A., Yogo, A., Tampo, M., Mori, M., Sakaki, H., Hayashi, Y., Nakamura, T., Pikuz Jr., S.A., Skobelev, I.Y., Gasilov, S.V., Giulietti, A., Cecchetti, C.A., Boldarev, A.S., Gasilov, V.A., Magunov, A., Kar, S., Borghesi, M., Bolton, P., Daido, H., Tajima, T., Kato, Y. & Bulanov, S.V. (2009). Submicron ionography of nanostructures using a femtosecond-laser-driven-cluster-based source. *Appl. Phys. Lett*. **95**, 101107.

Faenov, A.Y., Pikuz, T.A., Fukuda, Y., Skobelev, I.Y., Nakamura, T., Bulanov, S.V., Hayashi, Y., Kotaki, H., Pirozhkov, A.S., Kawachi, T., Chen, L.M., Zhang, L., Yan, W.C., Yuan, D.W., Mao, J.Y., Wang, Z.H., Fortov, V.E., Kato, Y. & Kando, M. (2013). Generation of quantum beams in large clusters irradiated by super-intense, high–contrast femtosecond laser pulses. *Contrib. Plasma Phys*. **53**, 148–160.

Faenov, A.Y., Pikuz, T.A. & Kodama, R. (2016*b*). Laser-driven particle acceleration towards radiobiology and medicine. In *High Resolution Ion and Electron Beam Radiography with Laser-Driven Clustered Sources* (Giulietti, A. ed.), Chapter 12, pp. 271–294. Heidelberg, New York: Springer.

Faenov, A.Y., Skobelev, I.Y., Magunov, A.I., Pikuz, T.A., Abdallah Jr., J., Junkel-Vives, G.C., Blasco, F., Dorchies, F., Stenz, C., Salin, F., Auguste, T., Dobosz, S., Monot, P., D'Oliveira, P., Hulin, S., Boldarev, A. & Gasilov, V.A. (2001). X-ray radiation properties of clusters heated by fs laser pulses. *Proc. SPIE* **4504**, 121–132.

Faenov, A.Y., Skobelev, I.Y., Pikuz, T.A., Pikuz, S.A., Fortov, V.E., Fukuda, Y., Hayashi, Y., Pirozhkov, A., Kotaki, H., Shimomura, T., Kiriyama, H., Kanazawa, S., Kato, Y., Colgan, J., Abdallah, J. & Kando, M. (2012). X-ray spectroscopy diagnoses of clusters surviving under prepulses of ultra-intense femtosecond laser pulse irradiation. *Laser Part. Beams* **30**, 481–488.

Frenkel, Y.I. (1955). *Kinetic Theory of Liquids*. New York: Dover publications, Inc.

Fukuda, Y., Akahane, Y., Aoyama, M., Inoue, N., Ueda, H., Kishimoto, Y., Yamakawa, K., Faenov, A.Y., Magunov, A.I., Pikuz, T.A., Skobelev, I.Y., Abdallah Jr., J., Csanak, G., Boldarev, A.S. & Gasilov, V.A. (2004*a*). Generation of X rays and energetic ions from superintense laser irradiation of micron-sized Ar clusters. *Laser Part. Beams* **22**, 215–220.

Fukuda, Y., Akahane, Y., Aoyama, M., Inoue, N., Ueda, H., Nakai, Y., Tsuji, K., Yamanaka, K., Hironaka, Y., Kishimura, H., Morishita, H., Kondo, K. & Nakamura, K.G. (2004*b*). Relativistic laser plasma from micron-sized argon clusters as a debris-free x-ray source for pulse x-ray diffraction. *Appl. Phys. Lett*. **85**, 5099–5101.

Fukuda, Y., Faenov, A.Y., Pikuz, T., Kando, M., Kotaki, H., Daito, I., Ma, J., Chen, L.M., Homma, T., Kawase, K., Kameshima, T., Kawachi, T., Daido, H., Kimura, T., Tajima, T., Kato, Y. & Bulanov, S.V. (2008). Soft x-ray source for nanostructure imaging using femtosecond-laser-irradiated clusters. *Appl. Phys. Lett*. **92**, 121110.

Fukuda, Y., Faenov, A.Y., Tampo, M., Pikuz, T.A., Nakamura, T., Kando, M., Hayashi, Y., Yogo, A., Sakaki, H., Kameshima, T., Pirozhkov, A.S., Ogura, K., Mori, M., Esirkepov, T.Z., Koga, J., Boldarev, A.S., Gasilov, V.A., Magunov, A.I., Yamauchi, T., Kodama, R., Bolton, P.R., Kato, Y., Tajima, T., Daido, H. & Bulanov, S.V. (2009). Energy increase in multi-MeV ion acceleration in the interaction of a short pulse laser with a cluster-gas target. *Phys. Rev. Lett*. **103**, 165002.

Fukuda, Y., Sakaki, H., Kanasaki, M., Yogo, A., Jinno, S., Tampo, M., Faenov, A., Pikuz, T., Hayashi, Y., Kando, M., Pirozhkov, A., Shimomura, T., Kiriyama, H., Kurashima, S., Kamiya, T., Oda, K., Yamauchi, T., Kondo, K. & Bulanov, S. (2013). Identification of high energy ions using backscattered particles in laser-driven ion acceleration with cluster-gas targets. *Radiat. Meas*. **50**, 92–96.

Fukuda, Y., Yamakawa, K., Akahane, Y., Aoyama, M., Inoue, N., Ueda, H., Abdallah Jr., J., Csanak, G., Faenov, A.Y., Magunov, A.I., Pikuz, T.A., Skobelev, I.Y., Boldarev, A.S. & Gasilov, V.A. (2003). X-ray study of microdroplet plasma formation under the action of superintense laser radiation. *JETP Lett*. **78**, 115–118.

Gasilov, S.V., Faenov, A.Y., Pikuz, T.A., Fukuda, Y., Kando, M., Kawachi, T., Skobelev, I.Y., Daido, H., Kato, Y. & Bulanov, S.V. (2009). Wide-field-of-view phase-contrast imaging of

https://doi.org/10.1017/S0263034617000350 Published online by Cambridge University Press

nanostructures with a comparatively large polychromatic soft x-ray plasma source. *Opt. Lett*. **34**, 3268–3270.

Gavrilenko, V.P., Faenov, A.Y., Magunov, A.I., Skobelev, I.Y., Pikuz, T.A., Kim, K.Y. & Milchberg, H.M. (2006). Observation of modulations in Lyman-α line profiles of multicharged ions in clusters irradiated by femtosecond laser pulses: Effect of a dynamic electric field. *Phys. Rev. A* **73**, 013203.

Hagena, O.F. (1992). Cluster ion sources. *Rev. Sci. Instrum*. **63**, 2374.

Hansen, S.B., Fournier, K.B., Faenov, A.Y., Magunov, A.I., Pikuz, T.A., Skobelev, I.Y., Fukuda, Y., Akahane, Y., Aoyama, M., Inoue, N., Ueda, H. & Yamakawa, K. (2005). Measurement of $2l-nl'$ x-ray transitions from ≈1 μm Kr clusters irradiated by high-intensity femtosecond laser pulses. *Phys. Rev. E* **71**, 016408.

Hayashi, Y., Fukuda, Y., Faenov, A.Y., Kando, M., Kawase, K., Pikuz, T.A., Homma, T., Daido, H. & Bulanov, S.V. (2010). Intense and reproducible *K*α emissions from micron-sized Kr cluster target irradiated with intense femtosecond laser pulses. *Japanese J. Appl. Phys*. **49**, 126401.

Hayashi, Y., Pirozhkov, A.S., Kando, M., Fukuda, Y., Faenov, A., Kawase, K., Pikuz, T., Nakamura, T., Kiriyama, H., Okada, H. & Bulanov, S.V. (2011). Efficient generation of Xe K-shell x rays by high-contrast interaction with submicrometer clusters. *Opt. Lett*. **36**, 1614–1616.

Jinno, S., Fukuda, Y., Sakaki, H., Yogo, A., Kanasaki, M., Kondo, K., Faenov, A.Y., Skobelev, I.Y., Pikuz, T.A., Boldarev, A.S. & Gasilov, V.A. (2013*a*). Characterization of submicron-sized CO_2 clusters formed with a supersonic expansion of a mixed-gas using a three-staged nozzle. *Appl. Phys. Lett*. **102**, 164103.

Jinno, S., Fukuda, Y., Sakaki, H., Yogo, A., Kanasaki, M., Kondo, K., Faenov, A.Y., Skobelev, I.Y., Pikuz, T.A., Boldarev, A.S. & Gasilov, V.A. (2013*b*). Mie scattering from submicron-sized CO_2 clusters formed in a supersonic expansion of a gas mixture. *Opt. Express* **21**, 20656–20674.

Junkel-Vives, G.C., Abdallah Jr., J., Auguste, T., D'Oliveira, P., Hulin, S., Monot, P., Dobosz, S., Faenov, A.Y., Magunov, A.I., Pikuz, T.A., Skobelev, I.Y., Boldarev, A.S. & Gasilov, V.A. (2002*a*). Spatially resolved x-ray spectroscopy investigation of femtosecond laser irradiated Ar clusters. *Phys. Rev. E* **65**, 036410.

Junkel-Vives, G.C., Abdallah Jr., J., Blasco, F., Dorchies, F., Caillaud, T., Bonte, C., Stenz, C., Salin, F., Faenov, A.Y., Magunov, A.I., Pikuz, T.A. & Skobelev, I.Y. (2002*b*). Evidence of supercritical density in 45-fs-laser-irradiated Ar-cluster plasmas. *Phys. Rev. A* **66**, 033204.

Kim, K.Y., Kumarappan, V. & Milchberg, H.M. (2003). Measurement of the average size and density of clusters in a gas jet. *Appl. Phys. Lett*. **83**, 3210–3212.

Kim, K.Y., Milchberg, H., Faenov, A.Y., Magunov, A.I., Pikuz, T.A. & Skobelev, I.Y. (2006). X-ray spectroscopy of 1 cm plasma channels produced by self-guided pulse propagation in elongated cluster jets. *Phys. Rev. E* **73**, 066403.

Koester, P., Bussolino, G.C., Cristoforetti, G., Faenov, A., Giulietti, A., Giulietti, D., Labate, L., Levato, T., Pikuz, T. & Gizzi, L.A. (2015). High-charge divergent electron beam generation from high-intensity laser interaction with a gas-cluster target. *Laser Part. Beams* **33**, 331–338.

Kugland, N.L., Constantin, C.G., Neumayer, P., Chung, H.-K., Collette, A., Dewald, E.L., Froula, D.H., Glenzer, S.H., Kemp, A., Kritcher, A.L., Ross, J.S. & Niemann, C. (2008). High *K*α x-ray conversion efficiency from extended source gas jet targets irradiated by ultra short laser pulses. *Appl. Phys. Lett*. **92**, 241504.

Oks, E., Dalimier, E., Faenov, A., Pikuz, T., Fukuda, Y., Andreev, A., Koga, J., Sakaki, H., Kotaki, H., Pirozhkov, A., Hayashi, Y., Skobelev, I., Pikuz, S., Kawachi, T., Kando, M., Kondo, K., Zhidkov, A. & Kodama, R. (2015). Revealing the second harmonic generation in a femtosecond laser-driven cluster-based plasma by analyzing shapes of Ar XVII spectral lines. *Opt. Express* **23**, 31991–32005.

Oks, E., Dalimier, E., Faenov, A.Y., Pikuz, T., Fukuda, Y., Jinno, S., Sakaki, H., Kotaki, H., Pirozhkov, A., Hayashi, Y., Skobelev, I., Kawachi, T., Kando, M. & Kondo, K. (2014). Two-plasmon decay instability's signature in spectral lines and spectroscopic measurements of charge exchange rate in a femtosecond laser-driven cluster-based plasma. *J. Phys. B: At. Mol. Opt. Phys*. **47**, 221001.

Parra, E., Alexeev, I., Fan, J., Kim, K.Y., McNaught, S.J. & Milchberg, H.M. (2000). X-ray and extreme ultraviolet emission induced by variable pulse-width irradiation of Ar and Kr clusters and droplets. *Phys. Rev. E* **62**, R5931.

Parra, E., McNaught, S.J., Fan, J. & Milchberg, H.M. (2003). Pump–probe studies of EUV and X-ray emission dynamics of laser-irradiated noble gas droplets. *Appl. Phys. A* **77**, 317–323.

Pikuz, T.A., Faenov, A.Y., Gasilov, S.V., Skobelev, I.Y., Fukuda, Y., Kando, M., Kotaki, H., Homma, T., Kawase, K., Hayahsi, Y., Kawachi, T., Daido, H., Kato, Y. & Bulanov, S. (2009). Propagation-based phase-contrast enhancement of nanostructure images using a debris-free femtosecond-laser-driven cluster-based plasma soft x-ray source and an LiF crystal detector. *Appl. Opt*. **48**, 6271–6276.

Rusek, M., Lagadec, H. & Blenski, T. (2000). Cluster explosion in an intense laser pulse: Thomas-Fermi model. *Phys. Rev. A* **63**, 013203.

Sherrill, M.E., Abdallah Jr., J., Csanak, G., Dodd, E.S., Fukuda, Y., Akahane, Y., Aoyama, M., Inoue, N., Ueda, H., Yamakawa, K., Faenov, A.Y., Magunov, A.I., Pikuz, T.A. & Skobelev, I.Y. (2006). Spectroscopic characterization of an ultrashort-pulse-laser-driven Ar cluster target incorporating both Boltzmann and particle-in-cell models. *Phys. Rev. E* **73**, 066404.

Skobelev, I.Y., Faenov, A.Y., Magunov, A.I., Pikuz, T.A., Boldarev, A.S., Gasilov, V.A., Abdallach Jr., J., Junkel-Vives, G.C., Auguste, T., Dobosz, S., d'Oliveira, P., Hulin, S., Monot, P., Blasco, F., Dorchies, F., Caillaud, T., Bonte, C., Stenz, C., Salin, F. & Loboda, P.A., Litvinenko, I.A., Popova, V.V., Baidin, G.V. & Sharkov, B.Y. (2002*a*). X-ray spectroscopy diagnostic of a plasma produced by femtosecond laser pulses irradiating a cluster target. *JETP* **94**, 966–976.

Skobelev, I.Y., Faenov, A.Y., Magunov, A.I., Pikuz, T.A., Boldarev, A.S., Gasilov, V.A., Abdallach Jr., J., Junkel-Vives, G.C., Auguste, T., d'Oliveira, P., Hulin, S., Monot, P., Blasco, F., Dorchies, F., Caillaud, T., Bonte, C., Stenz, C., Salin, F. & Sharkov, B.Y. (2002*b*). On the interaction of femtosecond laser pulses with cluster targets. *JETP* **94**, 73–83.

Sylla, F., Veltcheva, M., Kahaly, S., Flacco, A. & Malka, V. (2012). Development and characterization of very dense submillimetric gas jets for laser-plasma interaction. *Rev. Sci. Instrum*. **83**, 033507.

Tajima, T., Kishimoto, Y. & Downer, M.C. (1999). Optical properties of cluster plasma. *Phys. Plasmas* **6**, 3759.

Tao, Y., Hagmeijer, R., van der Weide, E.T.A., Bastiaens, H.M.J. & Boller, K.-J. (2016). Revisiting argon cluster formation in a

https://doi.org/10.1017/S0263034617000350 Published online by Cambridge University Press

planar gas jet for high-intensity laser matter interaction. *Appl. Phys*. **119**, 164901.

Zhang, L., Chen, L.-M., Wang, W.-M., Yan, W.-C., Yuan, D.-W., Mao, J.-Y., Wang, Z.-H., Liu, C., Shen, Z.-W., Li, Y.-T., Dong, Q.-L., Lu, X., Ma, J.-L., Faenov, A., Pikuz, T., Sheng, Z.-M. & Zhang, J. (2012). Electron acceleration via high contrast laser interacting with submicron clusters. *Appl. Phys. Lett*. **100**, 014104.

Zhang, L., Chen, L.-M., Yuan, D.-W., Yan, W.-C., Wang, Z.-H., Liu, C., Shen, Z.-W., Faenov, A., Pikuz, T., Skobelev, I., Gasilov, V., Boldarev, A., Mao, J.-Y., Li, Y.-T., Dong, Q.-L., Lu, X., Ma, J.-L., Wang, W.-M., Sheng, Z.-M. & Zhang, J. (2011). Enhanced K_α output of Ar and Kr using size optimized cluster target irradiated by high-contrast laser pulses. *Opt. Express* **19**, 25812–25822.

https://doi.org/10.1017/S0263034617000350 Published online by Cambridge University Press